Modeling temporal fluctuations in avalanching systems

M. Rypdal[1] and K. Rypdal[2]
[1]*Department of Mathematics and Statistics, University of Tromsø, Norway*
[2]*Department of Physics and Technology, University of Tromsø, Norway*
(Received 25 July 2008; published 26 November 2008)

We demonstrate how to model the toppling activity in avalanching systems by stochastic differential equations (SDEs). The theory is developed as a generalization of the classical mean-field approach to sandpile dynamics by formulating it as a generalization of Itô's SDE. This equation contains a fractional Gaussian noise term representing the branching of an avalanche into small active clusters and a drift term reflecting the tendency for small avalanches to grow and large avalanches to be constricted by the finite system size. If one defines avalanching to take place when the toppling activity exceeds a certain threshold, the stochastic model allows us to compute the avalanche exponents in the continum limit as functions of the Hurst exponent of the noise. The results are found to agree well with numerical simulations in the Bak-Tang-Wiesenfeld and Zhang sandpile models. The stochastic model also provides a method for computing the probability density functions of the fluctuations in the toppling activity itself. We show that the sandpiles do not belong to the class of phenomena giving rise to universal non-Gaussian probability density functions for the global activity. Moreover, we demonstrate essential differences between the fluctuations of total kinetic energy in a two-dimensional turbulence simulation and the toppling activity in sandpiles.

DOI: 10.1103/PhysRevE.78.051127 PACS number(s): 02.50.Ey, 05.65.+b, 45.70.Ht, 89.75.Da

I. INTRODUCTION

The aim of this paper is to present a consistent framework for the modelling of temporal fluctuations, including definition and computation of avalanche exponents, in sandpile (height) models such as the Bak-Tang-Wiesenfeld (BTW) and Zhang models [1,2]. One of the defining properties of self-organized criticality is that the probability density functions (PDFs) of avalanche duration and size are quantities subject to scaling—i.e., $p_{\mathrm{dur}}(\tau)\sim\tau^{-\alpha}$ and $p_{\mathrm{size}}(s)\sim s^{-\nu}$ [3,4]. The calculation of the exponents α and ν in the thermodynamic limit $N\to\infty$ (N^d is the number of sites in the d-dimensional lattice) has proven to be a difficult task in dimensions $d=2$ and $d=3$. This is partly due to the lack of simple finite-size scaling in models such as the BTW sandpile [3]. Moreover, it has recently been pointed out [5] that the difficulty may originate from the fact that the τ and s do not scale when defined in the traditional sense, which is to consider the duration of an avalanche as the time interval where toppling takes place between two successive zeros in the toppling activity. In this paper we shall denote avalanches defined this way as *type-I avalanches*.

The scaling property can be restored, however, if one defines the duration of an avalanche as the time interval when the toppling activity $x(t)$ exceeds a prescribed threshold x_{th}. We shall use the term *type-II avalanches* when the start and end of an avalanche is determined via such a threshold criterion. The idea of using a threshold on the toppling activity in the definition of avalanches was first introduced in [6], where it was argued that any avalanche analysis of real-world activity time series must define avalanches from a threshold, since there is no way to uniquely determine whether a non-negative continuous-valued experimental quantity is actually zero or just small. For type-II avalanches it can be shown by numerical simulation that the quiet times between avalanches in the BTW model are power-law distributed. For type-I avalanches the quiet times only depend on the statistics of the driver, which is usually assumed to be Poisson distributed.

The present work represents the first systematic investigation of type-II avalanche statistics for the BTW and Zhang sandpiles. We are particularly interested in the continuum limit where the system size $L=1$ is considered fixed and the spatial resolution increases as $N\to\infty$. The power-law statistics of avalanche observables have cutoffs for large avalanches due to the finiteness of the system, but as we increase the resolution, we see an increasing range of scaling for smaller avalanches. As $N\to\infty$, we keep the threshold fixed relative to the time-averaged activity $\langle x\rangle$, which scales as $\langle x\rangle\sim N^{D_1}$, where $0<D_1<2$. For the BTW sandpile, numerical simulation yields $D_1\approx 0.86$ [5]. This means that the number of overcritical sites corresponding to the threshold value diverges like $x_c\sim N^{D_1}$ in the limit $N\to\infty$.

We model the toppling activity in the continum limit by a stochastic differential equation [7] for a normalized toppling activity $X(t)$. In its simplest form this equation is in the form

$$dX(t)=\sigma\sqrt{X(t)}dW(t), \tag{1}$$

where $W(t)$ is the Wiener process. Without the factor $\sqrt{X(t)}$ on the right-hand side we would simply have that $X(t)=\sigma W(t)+X_0$ is a Brownian motion with diffusion coefficient $D=\sigma^2/2$. This factor, however, gives rise to a nonuniform (X-dependent) diffusion coefficient $D=\sigma^2X(t)/2$, and the stochastic process $X(t)$ will have nonstationary increments. This model can be perceived as a continuous version of the classical mean-field theory of sandpiles [8]. We use its corresponding Fokker-Planck equation to derive that $\alpha=2$ and $\nu=3/2$ when avalanches are defined in the type-I sense. This is the same result obtained by mean-field theory [3,4,8]. For type-II avalanches the effect of the nonuniform diffusion coefficient vanishes for avalanches of durations short compared

to that of a system-size avalanche, and for the purposes of calculating α and ν we can assume that the the toppling activity is a standard Brownian motion. Solving the Fokker-Planck equation for Brownian motion (or equivalently using the known distribution of first return times in Brownian motion) we obtain $\alpha=3/2$ and $\nu=4/3$.

For the modeling of nontrivial sandpile models (BTW and Zhang) the stochastic differential equation takes the form

$$dX(t) = f(X)dt + \sigma\sqrt{X(t)}dW_H(t). \tag{2}$$

Two important generalizations of the stochastic model are included here. First, from numerical simulations of sandpiles we find that for small activities $X(t)$ there is an effective positive drift term. This term is dominant for very small activity, since the diffusion term is negligible for very small $X(t)$ due to the X factor in the diffusion coefficient. The positive drift term is X dependent and quickly decreases as X increases, but strongly influences the avalanche statistics because it contributes to prevent avalanches from terminating when $X(t)$ approaches zero. We believe that this effect is responsible for destroying the scaling of avalanche duration and size (when these are defined in the type-I sense). However, if the drift term is small compared to the diffusion term for $X>X_{th}$, the drift term will not affect the avalanche statistics if one employs a threshold X_{th} to define type-II avalanches. This explains why scaling of size and duration is restored when when type-II avalanches are introduced. Another generalization, which is essential for the avalanche statistics, is the Hurst exponent H of the noise term. The mean-field approach to sandpiles implicitly assumes that $H=1/2$. However, this is not the case for the BTW and Zhang models. Actually, analysis of numerical simulations of the sandpiles shows that $H=0.37$ for the BTW model and $H=0.75$ for the Zhang model.

As in the mean-field model, the effect of the nonuniform diffusion coefficient vanishes as the threshold increases. Hence, by keeping the threshold X_{th} fixed and increasing N we can, for the purposes of computing α and ν for avalanches where X never grows much greater than X_{th}, consider the toppling activity as a fractional Browian motion. Using the result of Ding and Yang [9], that the PDF for the first return time in fractional Brownian motion scales like $\sim\tau^{H-2}$, we obtain the general results $\alpha=2-H$ and $\nu=2/(1+H)$ (see Refs. [10,11]).

Although the drift term and the nonuniformity of the diffusion coefficient are not important to calculate the avalanche exponents for type-II avalanches whose duration are short enough not to be limited by the finite system size, they are important on time scales where the toppling activity is a stationary process. These are scales sufficiently long that the toppling activity of avalanches is limited by the boundaries. The stochastic equation (2) is fully equipped to handle these time scales. A good example of the applicability of these aspects of the stochastic model is the computation of the PDF for the temporal fluctuations in the activity signal itself.

For weakly driven sandpiles the PDFs of the fluctuations in the toppling activity are stretched exponentials. This result is reproduced by simulation of the stochastic model [5]. For stronger driving the activity exhibits fluctuations which are more confined around a mean value where the drive and dissipation balance each other. It has been claimed that the PDFs of the toppling activity in sandpiles are examples of universal Bramwell-Holdsworth-Pinton (BHP) distributions [12,13], a certain class of asymmetric PDFs commonly seen in complex systems. Our sandpile simulations show that the BHP distributions can only be seen if one fine-tunes the driving rate to a certain value, and for other driving rates the PDFs belong to a much wider class of distributions. For sufficiently strong drive Gaussian PDFs are observed. These can also be obtained from the stochastic model if one correctly models the drift term in this parameter range.

The rest of the paper is structured as follows: In Sec. II we explain and derive the stochastic model for the toppling activity. In Sec. III we compute the avalanche exponents for type-I and type-II avalanches for the mean-field case ($H=1/2$) by solving a Fokker-Planck equation, and for $H\neq 1/2$ we compute the avalanche exponents for type-II avalanches as a function of H. The results allow us to predict the avalanche exponents for sandpile models by computation of the Hurst exponents. These results are then tested against numerical simulations of the BTW and Zhang models and are shown to agree well. In Sec. IV we present results which indicate that type-II avalanches exhibit so-called finite-size scaling, even though type-I avalanches do not.

In Sec. V we use the stochastic theory to calculate the PDFs of the toppling activity signal, both for strongly driven sandpiles and in the weak driving limit. The method is finally applied to the fluctuations in kinetic energy in a two-dimensional (2D) turbulence simulation. In this case the process is given by a different kind of stochastic differential equation

$$dX(t) = bdt + ce^{aX}dW(t). \tag{3}$$

This equation gives rise to a Fischer-Tippet-Gumbel distribution [14,15], which is very close to the BHP distribution. The differences between the stochastic models for sandpile activity and kinetic energy fluctuations in 2D turbulence may represent an essential distinguishing feature between 2D turbulent dynamics and the kind of avalanching dynamics which are observed in the classical sandpile models.

In Sec. VI we summarize and conclude the work.

II. STOCHASTIC MODEL

Let $x(k)$ denote the number of overcritical sites at time step k in a sandpile. A common feature of (height-type) sandpile models is that the typical size of increments Δx is proportional to the square root of the toppling activity x. To be more precise, the conditional probability of an increment $\Delta x(k)=x(k+1)-x(k)$, given $x=x(k)$, is

$$P(\Delta x|x) = \frac{1}{\sqrt{2\pi\sigma^2 x}}\exp\left(-\frac{\Delta x^2}{2\sigma^2 x}\right). \tag{4}$$

In Fig. 1 this property is verified for the BTW model (it holds in the Zhang model as well). This result can be explained as follows: At a given time k there are $x=x(k)$ overcritical sites, which we can enumerate $i=1,2,\ldots,x$. In the

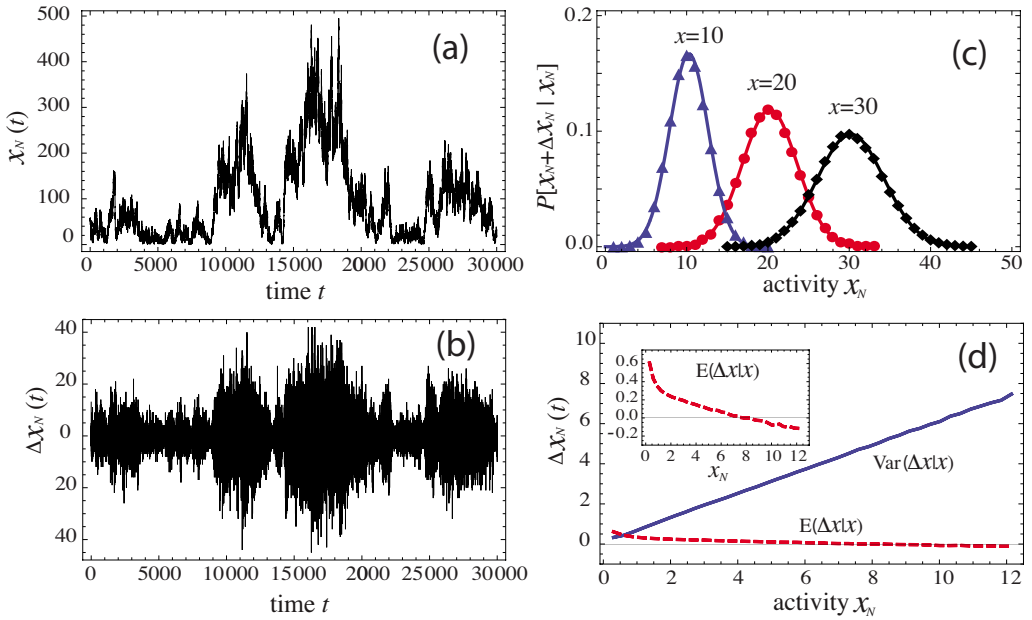

FIG. 1. (Color online) (a) A realization of the toppling activity $x(k)$ in the BTW sandpile. (b) The increments $\Delta x(k)=x(k+1)-x(k)$ of the trace in (a), showing that $\Delta x(k)$ is large when $x(k)$ is large. (c) Conditional PDFs of $x+\Delta x$ for $x=10,20,30$, respectively. (d) The conditional mean and variance of Δx versus x. Time is measured in units of the discrete time steps in the code.

next time step $k\to k+1$ each site i distributes energy to its neighbors and will usually (always in the BTW model) become subcritical. If none of the neighbors receive sufficient energy to become overcritical, the contribution to Δx from site i is $\xi_i=-1$. If exactly one of the neighbors become overcritical, then $\xi_i=0$ and so on. For the two-dimensional models the maximal value of ξ_i is 4 (3 for the BTW model) since a site maximally can excite four neighboring sites. Hence, for this case, we consider ξ_i to be random variables with realizations in $\{-1,0,1,2,3,4\}$. The randomness originates from the local configuration in the vicinity of the overcritical site; i.e., as an approximation we consider the different realizations of ξ_i (at a fixed time k) as independent of each other. We also consider the distribution of ξ_i to be identical for all overcritical sites and for all times. In this approximation the total increment Δx can be written as a sum of independent, identically distributed, random variables $\Delta x=\xi_1+\cdots+\xi_x$, and by the central-limit theorem we have (4) provided that the local means $\langle\xi\rangle$ are zero. Then $\sigma^2=\langle\xi^2\rangle=(-1)^2p_{-1}+\cdots+4^2p_4$, where $\mathbf{p}=(p_{-1},\ldots,p_4)$ is the probability vector for the local increment processes.

If the local processes at different times k are independent of each other, then $x(k)$ is a Markov process which satisfies a stochastic difference equation

$$\Delta x(k)=\sigma\sqrt{x(k)}w(k),$$

where $w(k)$ is a stationary, normalized, and uncorrelated Gaussian process—i.e., $w(k)=W(k+1)-W(k)$, where $W(t)$ is the Wiener process. Under a rescaling of time $t=k\delta t$ and $X(t)=x(k)\delta x$ we have

$$\begin{aligned}\Delta X(t)&=X(t+\delta t)-X(t)=\delta x[x(k+1)-x(k)]\\&=\delta x^{1/2}\sigma\sqrt{X(t)}[W(k+1)-W(k)]\\&=\left(\frac{\delta x}{\delta t}\right)^{1/2}\sigma\sqrt{X(t)}[W(t+\delta t)-W(t)].\end{aligned}$$

In the last step we used the self-affinity of the Wiener process, $W(t/\delta t)\overset{d}{=}\delta t^{-1/2}W(t)$. For $\delta x=\delta t$ we have a well-defined model in the limit δt, $\delta x\to 0$: namely, the Itô stochastic differential equation (1).

The first generalization of this model is obtained if we relax the requirement that the local increment processes $\xi_i(k)$ at time k be independent of the local increment processes $\xi_j(k')$, $j=1,\ldots,x(k')$, at previous times $k'<k$. In this case we need to model memory effects in the stationary Gaussian process

$$w(k)=\frac{\Delta x(k)}{\sigma\sqrt{x(k)}}.$$

From the power spectrum or the variogram of the activity signal from numerical simulation of the BTW and Zhang models we find that $w(k)$ can be accurately modeled as a colored noise characterized by a Hurst exponent H. That is, $w(k)=W_H(k+1)-W_H(k)$, with W_H being a normalized (diffusion coefficient=1) fractional Brownian motion (FBM). If we perform the rescaling $t=k\delta t$ and $X(t)=x(k)\delta x$ in the case $H\neq 1/2$, we obtain

$$\Delta X(t)=\left(\frac{\delta x}{\delta t^{2H}}\right)^{1/2}\sigma\sqrt{X(t)}[W_H(t+\delta t)-W_H(t)],$$

and by requiring that $\delta x=\delta t^h$, with $h=2H$, we obtain the stochastic differential equation

$$dX(t)=\sigma\sqrt{X(t)}dW_H(t). \tag{5}$$

If we assume that the the stochastic process $X(t)$ is self-affine with self-affinity exponent h—i.e., $X(st)\overset{d}{=}s^hX(t)$—it is easy to verify that Eq. (5) is invariant with respect to the transformation $t\to st$ if $h=2H$ (see Fig. 2). Thus, the exponent h

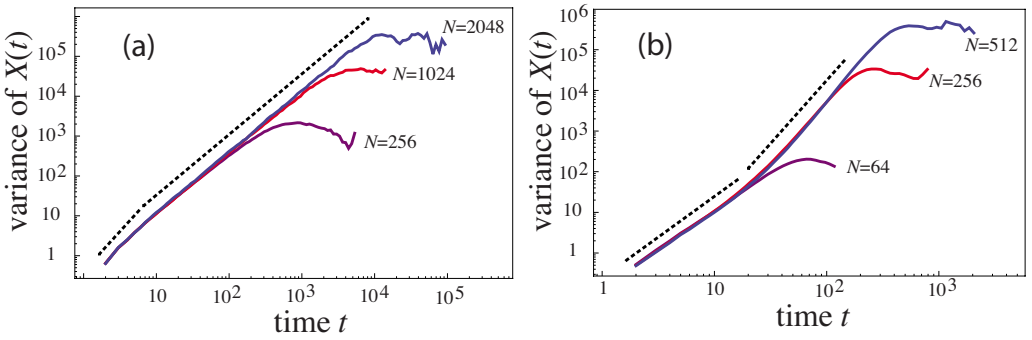

FIG. 2. (Color online) (a) Determining $h=2H$ in the BTW model through the calculation of the variance of the activity $X(k)$ in avalanches still running at time t. On very short time scales there is a Hurst exponent $H=0.5$ (the first dashed line has slope $2h=4H=2$); on longer time scales the Hurst exponent is $H=0.37$ (the second dashed line has slope $2h=4H=1.5$). (b) Determining $h=2H$ in the Zhang model by the same method as in (a). In this case we again have $H\approx 0.5$ for short times, but $H=0.75$ for longer times. Time is measured in units of the discrete time steps in the code.

$=2H$ is the self-affinity exponent of the process $X(t)$, where H is the Hurst exponent determining the color of the noise process driving the stochastic differential equation. Observe that the reason why $h\neq H$ is the nonstationarity of the increment process due to the the factor $\sqrt{X(t)}$ in Eq. (5). Note also that the case $H=1/2$ corresponds to $h=1$.

The self-affinity of $X(t)$ described by Eq. (5) implies that there is no upper bound on the fluctuations on increasing time scales; i.e., Eq. (5) describes the activity of an infinite sandpile where the activity is never influenced by the system boundaries. From a physical viewpoint, however, it is more interesting to consider the dynamics of a finite sandpile in the continuum (thermodynamic) limit, and for this purpose it is natural to let the scaling factor δx depend on N such that $X_N=x_N\delta x(N)$ is bounded in the limit $N\to\infty$—for instance, such that $\lim_{N\to\infty}\max(X_N)=1$. Such a bound on $X(t)$ can be obtained by the introduction of a drift term $f(X)dt$ leaving the stochastic equation in the form of Eq. (2), where $f(X)$ is negative for large X. The form of $f(X)$ can be found from sandpile simulations by computing the conditional mean $E(\Delta x|x)$ of the increments and is shown in Fig. 1(d). It appears that $f(X)$ is a decreasing function, positive for small X and negative for large X, and $f(X)=0$ for a characteristic activity $X_c\sim 1$. Without the stochastic term the drift term establishes X_c as a stable fixed point for the dynamics.

Since $f(X=0)>0$, solutions of Eq. (2) with initial condition $X(0)>0$ exist and are positive for all $t>0$. This means that while Eq. (5) has solutions for which $X(t)=0$ after a finite time (avalanches terminate), avalanches described by Eq. (2) will never terminate in the meaning $X(t)=0$ (type-I avalanches). This signifies that type-I termination never occurs in the continuum limit. If sandpiles of increasing N are simulated and the type-I avalanche durations are computed in the rescaled coordinates, the durations generally grow without bounds for increasing N. The reason is that the effective threshold for type-I termination in a discrete sandpile is $x_N=1$, but in rescaled coordinates this threshold $X_N=x_N\delta x(N)$ goes to zero as $N\to\infty$. As this rescaled threshold vanishes, the duration in rescaled time goes to infinity. Since the type-I termination is a discreteness effect, the resulting PDFs of avalanche durations depend on N (system discreteness) and are not power laws. As we shall demonstrate later, the introduction of activity thresholds which are defined in the rescaled coordinates, and hence remain finite in the continuum limit, will give rise to PDFs of durations of type-II avalanches which converge to a specific power-law in this limit.

Equation (2) remains valid also for sandpiles which are driven by continuous feeding of sand during avalanches. The drive adds a positive contribution to the drift function $f(X)$ for $X<X_c$, but a negative contribution for $X>X_c$, because for large activites $f(X)$ mainly accounts for the increased boundary losses. The result is a steeper $f(X)$, which tends to confine the activity closer to the fixed point X_c. On the other hand, the increased drive also increases the diffusion coefficient (by increasing σ) due to a larger number of new active clusters initiated per unit time. The net effect is a positive shift of X_c and that the fluctuations in X are confined to a smaller region around X_c. For sufficiently strong drive the range of variation in $X(t)$ becomes so small that the diffusion coefficient does not vary much. It is nevertheless important to model it correctly in order to calculate the PDFs of the fluctuations in toppling activity.

III. CALCULATION OF AVALANCHE EXPONENTS

We denote the stochastic model Eq. (1) [which is Eq. (2) with $H=1/2$ and $f(X)=0$] the *mean-field model* of sandpiles. This is because its underlying assumptions and the results derived from it coincide with what is known as the mean-field solution of sandpiles in the literature [8]. Equation (1), together with its corresponding Fokker-Planck formulation, can be used to calculate the avalanche exponents α and ν. The idea is that each avalanche corresponds to a realization $X(t)$ with some initial condition $X(0)=X_0$ ($X_0\ll X_{max}$). The avalanche propagates until the realization $X(t)$ terminates at $t=t_1$ in the meaning that $X(t)>0$ for $t<t_1$ and $X(t_1)=0$. Calculating the ratio of surviving realizations at different times t in an ensemble will provide information about the distribution of avalanche durations. The avalanche size distribution can then be obtained by using a general relationship between the exponent ν, the self-affinity exponent $h=2H=1$, and the duration exponent α [Eq. (10) below].

The scenario outlined above can be mathematically formulated as follows: Let $P(X,t)dX$ be the probability that $X(t)$ exists (avalanche lives longer than t) and that $X(t) \in (X, X+dX)$. Then the the probability $\rho(t)$ that an avalanche still runs after a time t (we call it the survival function) is given by

$$\rho(t) = \int_0^\infty P(X,t)dX, \tag{6}$$

and the probability density function for durations is $p_{\mathrm{dur}}(\tau) = -\rho'(\tau)$. The density $P(X,t)$ can be calculated by solving the Fokker-Planck equation

$$\frac{\partial P}{\partial t} = \frac{\sigma^2}{2}\frac{\partial^2}{\partial X^2}(XP) \tag{7}$$

on $X \in [0,\infty)$, $t \in [0,\infty)$, subject to an absorbing boundary condition $\lim_{X\to 0} XP(X,t)=0$ and an initial condition $P(X,0)=\delta(X-X_0)$.

To correctly incorporate the absorbing boundary condition we let $U=XP$ and solve the corresponding Fokker-Planck equation for U with boundary condition $U(0)=0$ to get

$$P(X,t) = \int_0^\infty G(X,Y,t)P(Y,0)dY,$$

where

$$G(X,Y,t) = \sqrt{\frac{Y}{4X}}\int_0^\infty J_1(s\sqrt{Y})J_1(s\sqrt{X})e^{-(\sigma^2 s^2/8)t}sds.$$

Remark 1. The most elegant way to obtain the solution is to use the integral transform pair

$$\hat{F}(s) = \frac{1}{2}\int_0^\infty F(X)J_1(s\sqrt{X})\sqrt{X}dX,$$

$$F(X) = \frac{1}{\sqrt{X}}\int_0^\infty \hat{F}(s)J_1(s\sqrt{X})sds.$$

Taking the transform of the Fokker-Planck equation we obtain the ordinary differential equation (ODE)

$$\frac{\partial \hat{P}}{\partial t}(s,t) = -\frac{\sigma^2 s^2}{4}\hat{P}(s,t),$$

which we can solve and take the inverse transform. It is also easy to solve the Fokker-Planck equation for $U=XP$ by separation of variables.

If $P(X,0)=\delta(X-X_0)$, the solution of the absorbing boundary problem is $P(X,t)=G(X,X_0,t)$. Moreover,

$$\lim_{X\to 0} P(X,t) = \frac{\sqrt{X_0}}{4}\int_0^\infty s^2 J_1(s\sqrt{X_0})\exp\left(-\frac{\sigma^2 s^2}{8}t\right)ds$$

$$= \frac{4X_0}{\sigma^4 t^2}\exp\left(-\frac{2X_0}{\sigma^2 t}\right). \tag{8}$$

From Eqs. (6)–(8) and the absorbing boundary condition at $X=0$ we find that

$$\frac{d\rho}{dt} = -\frac{\sigma^2}{2}\lim_{X\to 0} P(X,t) = -\frac{2X_0}{\sigma^2 t^2}\exp\left(-\frac{2X_0}{\sigma^2 t}\right).$$

Hence the PDF for avalanche durations τ is

$$p_{\mathrm{dur}}(\tau) = \frac{2X_0}{\sigma^2\tau^2}\exp\left(-\frac{2X_0}{\sigma^2\tau}\right),$$

and for $\tau \gg 2X_0/\sigma^2$ we have $p_{\mathrm{dur}}(\tau) \sim \tau^{-\alpha}$, $\alpha=2$.

This result crucially depends on the correct formulation of the Fokker-Planck equation. If the stochastic process $X(t)$ were a classical Brownan motion, the Fokker-Planck equation would have the form of the standard heat equation, and by performing the analogous calculations for this equation we get $p_{\mathrm{dur}}(\tau) \sim \tau^{-3/2}$. The same scaling relation ($\sim\tau^{3/2}$) is obtained if one (incorrectly) employs the Stratonovich formulation of the Fokker-Planck equation rather than the Itô form [7].

From the derivation of the stochastic model we have seen that the process $X(t)$ has a self-affinity exponent $h=2H$ (for $H=1/2$ we have $h=1$). This means that $X(t)$ disperses like $\sim t^h$. For long avalanches this implies that the size of the avalanche scales as

$$s = \int_0^\tau X(t)dt \sim \int^\tau t^h dt \sim \tau^{h+1}. \tag{9}$$

This property is easy to check directly by studying the relation between duration and sizes of avalanches in sandpiles. We find that the relation holds for large avalanches, whereas for very small avalanches $s \sim \tau^1$. If the survival function scales as $\rho(\tau) \sim \tau^{-\delta} = \tau^{-\alpha+1}$, then using (9) together with $p_{\mathrm{size}}(s)ds = p_{\mathrm{dur}}(\tau)d\tau$ yields that if $p_{\mathrm{size}}(s) \sim s^{-\nu}$, then

$$\nu = \frac{1+h+\delta}{1+h} = \frac{\alpha+h}{1+h}. \tag{10}$$

In the case $H=1/2$ ($h=1$) and $\alpha=2$ this gives $\nu=3/2$. This mean-field solution is known to be quite correct for the random neighbor sandpile model [16], but numerical simulation shows that is fails for type-I as well as type-II avalanches in the BTW and Zhang models. The computation of these exponents is shown for these models in Figs. 3 and 4 below. The computation of h presented in Fig. 2, for type-I avalanches yields $H=h/2=0.37$ for the BTW model and $H=0.75$ for the Zhang model. This invalidates the Fokker-Planck formulation, which can be strictly justified only for a white noise source term ($H=1/2$). This is one reason for the failure of the mean-field approach, but there are also others, as will be discussed in the following.

For avalanche duration and size type-I avalanches do not yield good power-law PDFs. The reason for this was discussed in the previous section: letting avalanches terminate when $x_N(t)=0$ in a sandpile with N^d sites corresponds to using an effective threshold for termination in the rescaled coordinates $X_N(t)$, which goes to zero as $N\to\infty$. The termination process depends on the discreteness of the system, and one cannot expect convergence to scale-invariant behavior in the continuum limit.

For type-II avalanches Figs. 3 and 4, below, show good scaling for duration and size in BTW and Zhang models, but

TABLE I. Exponents in mean-field solutions ($H=1/2$) of the stochastic equation with zero threshold (type-I) and large threshold (type-II).

	Type-I avalanches	Type-II avalanches)
H	1/2	1/2
h	1	1/2
α	2	3/2
ν	3/2	5/4

the scaling exponents differ from those of the mean-field approach. The discrepancy is partly due to the fact that the sandpile models have $H \neq 1/2$, but is also related to the observation that the introduction of a finite termination threshold X_{th} modifies the exponent h as it appears in Eqs. (9) and (10). In the following we shall demonstrate that it is possible to obtain analytical results for type-II avalanches from the stochastic model which are in agreement with the corresponding sandpile simulations.

First we observe that omission of the drift term will only have effect on avalanches which are so large that they are strongly limited by boundary dissipation. Next, we notice that the effect of the positive drift term for small activities is eliminated for type-II avalanches if $X_{th} > X_c$. In other words, it is only the cutoffs of the power-law PDFs due to finite system size which are lost by this omission. Thus, by considering a threshold X_{th} which is not much smaller than the mean activity $\langle X \rangle$ and considering only avalanches which are sufficiently small not to be influenced by the boundary dissipation, we have $X(t) \sim X_{th}$ and thus can justify the substitution $X(t) \to X_{th}(t)$ on the right-hand side in Eq. (5). This equation then reduces to the equation for an FBM with Hurst exponent H. For an FBM the duration of avalanches is given by the return time statistics for $W_H(t)$, which is known to scale like τ^{H-2} [9]; i.e., we have

$$\alpha = 2 - H. \tag{11}$$

Now we need to address a slightly subtle point: the exponent h, as defined in Eq. (9), is $h=2H$ for times τ so large that $X(\tau) \gg X(0)$. Only on such time scales will the effect of the factor $\sqrt{X(t)}$ in the stochastic term show up in the scaling. However, this makes sense only for type-I avalanches where we can choose $X(0) \ll \langle X \rangle$. For type-II avalanches we have $X(0) \approx X_{th}$, and it is more natural to consider the opposite limit where τ is so small that $\hat{X}(\tau) \equiv X(\tau) - X_{th} \ll X(0) \approx X_{th}$. On these time scales the activity measured relative to the threshold level scales like an FBM with Hurst exponent H—i.e., $\hat{X}(t) \sim t^H$—because $X(t) \approx X_{th}$. The avalanche size of type-II avalanches defined as $\hat{s}(\tau) \equiv \int_0^\tau \hat{X}(t) dt$ then scales as $\sim \tau^{1+H}$. Thus, for type-II avalanches we have $h=H$, and hence Eq. (10) for this case reduces to

$$\nu = \frac{2}{1+H}. \tag{12}$$

In the mean-field limit $H=1/2$ these exponents reduce to those given on the right-hand column in Table I. These results, obtained analytically by approximating the coefficient on the right-hand side in the stochastic equation by its threshold value, have been verified by numerical solutions of the full equation. Similar results for fractional Brownian motion have been obtained in [10,11].

Equations (11) and (12) show that the calculations of α and ν reduce to determining the Hurst exponent of the normalized increment process

$$w(k) = \frac{\Delta x(k)}{\sqrt{x(k)}},$$

which can easily be constructed from the toppling activity signal. The corresponding Hurst exponent of the motion,

$$W(k) = \sum_{i=0}^{k} w(k),$$

can be calculated using standard techniques such as taking the power spectrum or constructing variograms. Alternatively we can find H by computing the variance of $X(t)$ in an ensemble of realizations starting with small initial values of X. This variance scales like $\langle X^2(t) \rangle \sim t^{2h} = t^{4H}$. Figure 2 shows this computation for the BTW and Zhang models. Since we find $H=0.37$ for the BTW model, the type-II scaling exponents are $\alpha=1.63$ and $\nu=1.49$. This is verified by numerical calculation of α and ν using a threshold $\langle x \rangle/3$, as shown in Fig. 3.

In the Zhang model the process $w(k)$ is more complicated. Figure 4 shows that $W(k)$ has a Hurst exponent $H=0.5$ on short time scales and a different Hurst exponent $H=0.75$ on longer time scales. This means that short avalanches should satisfy the mean-field solution $\alpha=1.5$ and $\nu=1.33$, whereas longer avalanches should have exponents $\alpha=1.25$ and $\nu=1.14$. All of these predictions are verified by the direct calculation of α and ν as shown in Fig. 4.

For increasing N the long-avalanche scaling dominates an increasing portion of the graph, so in the continuum limit the mean-field solution only prevails at infinitely small scales in rescaled coordinates. It is, however, a nice verification of our method to see that the relation between the avalanche exponents and the Hurst exponent correctly predicts the avalanche exponents on short time scales as well. These results on the BTW and Zhang models are summarized in Table II.

Remark 2. The numerical simulations of the Zhang model are run using the standard toppling rule $z_i \to 0$ and $z_j \to z_i + z_i/4$ if z_i is overcritical and j is a nearest neighbor of i. Whenever the configuration has no overcritical sites a random site i is chosen with respect to uniform probability and a mass ϵ is added to this site: $z_i = z_i + \epsilon$. In the simulations presented in this paper we use $\epsilon=0.1$. In the strongly driven Zhang models presented in Sec. V the feeding times (which can now be during avalanches) are Poisson distributed and we have used $\epsilon=0.25$. For the BTW model we have used the standard toppling rule $z_i \to z_i - 4$ and $z_j = z_j + 1$ throughout the paper. As usual, a mass $\epsilon=1$ is added to a random site whenever the configuration is stable.

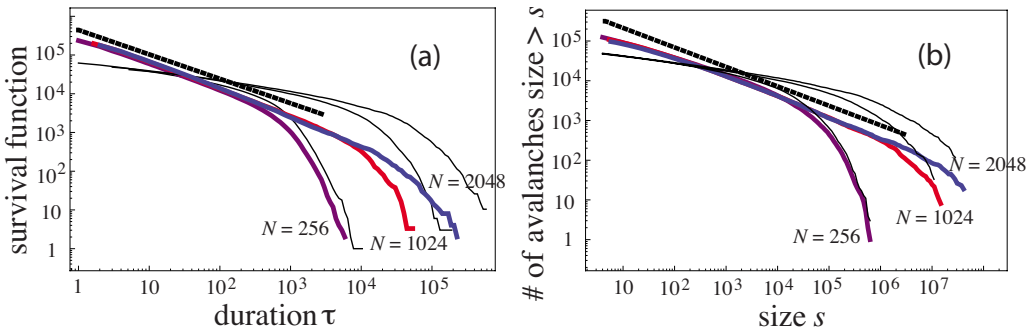

FIG. 3. (Color online) (a) The survival function of avalanches in the BTW model computed with thresholds $\langle X\rangle/3$ (type-II, thick curves) and without thresholds (type-I, thin curves). The dashed line corresponds to $\alpha=2-H=1.63$. (b) The probability density function of avalanches with size $>s$ in the BTW model computed with thresholds (thick curves) $\langle X\rangle/3$ and without thresholds (thin curves). The dashed line corresponds to $\nu=2/(1+H)=1.49$.

IV. FINITE-SIZE SCALING FOR TYPE-II AVALANCHES

A systematic technique for the determination of the avalanche exponents α and ν is the so called moment analysis [3]. We illustrate how this works for the size distribution of the BTW model. The analysis confirms our result $\nu=0.49$ for the BTW model for type-II avalanches. Let $p_{\text{size}}(s;N)$ be the PDF of avalanche size s in the two-dimensional BTW model with N^2 sites and a threshold $\langle x\rangle/3$. Let us assume finite-size scaling (FSS). This means that for $N,s\gg 1$ we have

$$p_{\text{size}}(s;N) \propto s^{-\nu}G(s/N^D), \tag{13}$$

for some exponent $D>0$, where $G(r)$ falls off quickly for $r>1$. From Eq. (13) we observe that

$$\langle s^q\rangle \propto N^{D(1+q-\nu)}\int_{1/N^D}^{\infty} r^{q-\nu}G(r)dr.$$

The integral tends to a constant as $N\to\infty$, so we have $\langle s^q\rangle \sim N^{D(1+q-\nu)}$. Thus, if we plot $\langle s^q\rangle$ versus N in a log-log plot, the slope of a fitted straight line will give us an estimate of the exponent $\zeta(q)=D(1+q-\nu)$ for $q=1,2,3,\ldots$. Figure 5(a) shows the computation of moments of s as a function of N for type-II avalanches obtained from simulation of the BTW model, and Fig. 5(b) shows the exponent $\zeta(q)$ versus q. We find that $\zeta(q)\sim q^{2.81}$, hence that $D=2.81$. Moreover, when plotted in a log-log plot, the intersection of $\zeta(q)$ with the first axis corresponds to the value $\nu-1$. Hence, based on our predictions, this intersection should be in the point 0.49. This value is plotted as a dotted vertical line in Fig. 5(b), confirming our result with good accuracy.

Strictly, this method requires that we have data collapse when rescaling the avalanche sizes by s/N^D. The shape of the scaling function $G(r)$ can be seen by plotting $s^{\nu}p_{\text{size}}(s;N)$ versus s/N^D. This is shown in Fig. 6. The data collapse for the available system sizes is not perfect, but it is better than for type-I avalanches. In fact, it seems that we might have convergence to an N-independent scaling function as $N\to\infty$ and that the lack of data collapse observed here is simply due to the fact that we are not able to simulate sufficiently large sandpiles. Thus the general lack of scaling for for type-I avalanches, including the finite-size scaling, seems to be restored for type-II avalanches.

V. PDFs OF THE TOPPLING ACTIVITY

When calculating the PDFs of the toppling activity signal we have to distinguish between the weakly and strongly driven sandpiles. For the weakly driven sandpiles the toppling activity covers a large range and the high-activity tail of the PDF decays like a stretched exponential. This property

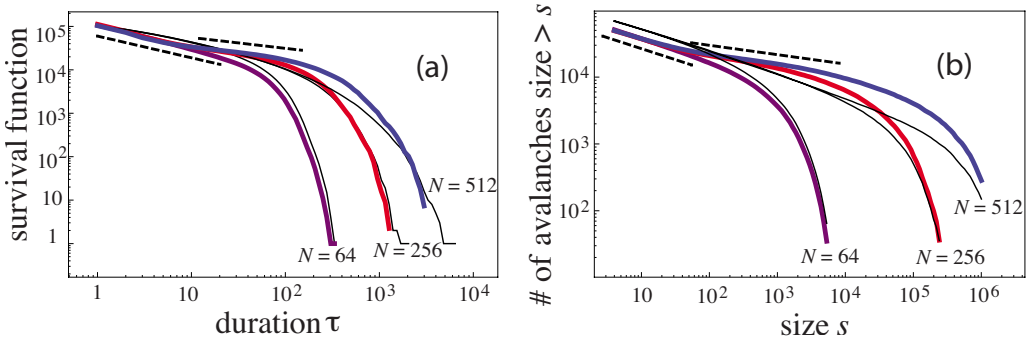

FIG. 4. (Color online) (a) The probability of having avalanches of duration $>\tau$ in the Zhang model computed with thresholds $\langle X\rangle/3$ (thick curves) and without thresholds (thin curves). The first dashed line corresponds to $\alpha=2-H=1.50$ obtained with $H=0.50$, and the second dashed line corresponds to $\alpha=2-H=1.25$ obtained with $H=0.75$. (b) The probability of having avalanches with size $>s$ in the Zhang model computed with thresholds $\langle X\rangle/3$ (thick curves) and without thresholds (thin curves). The first dashed line corresponds to $\nu=2/(1+H)=1.33$ obtained with $H=0.50$, and the second dashed line corresponds to $\nu=2/(1+H)=1.14$ obtained with $H=0.75$.

TABLE II. Exponents for type-II avalanches computed from $H=0.37$ in the BTW model and $H=0.50$ (short time scales) and $H=0.75$ (long time scales) in the Zhang model.

	BTW	Zhang (short times)	Zhang (long times)
H	0.37	0.50	0.75
α	1.63	1.50	1.25
ν	1.49	1.33	1.14

can be reproduced by simulations of Eq. (2) where $f(X)$ decays exponentially to zero as X increases. Figure 7 compares the PDF obtained from such a simulation of the stochastic differential equation (run with $H=0.37$) with the PDF of the weakly driven BTW model. The stochastic model is run by initiating new avalanches (realizations) whenever the previous avalanche terminates, thus representing the classical slow drive of the sandpile model. Since the Hurst exponents of the Zhang and BTW models are different from $1/2$, the application of the Fokker-Planck equation cannot be used to calculate the shape of the PDFs, and thus we have to rely on numerical simulations.

It is also interesting to study the PDFs of toppling activity in strongly driven sandpiles—in particular, in light of recent claims that this toppling activity belongs to a class of fluctuating global quantities with a universal non-Gaussian shape [12,13]. These PDFs are reminiscent of distributions derived from the extreme value theory of statistics [14,15], which deals with a sequence of n identically distributed, independent random variables $y_1,\ldots,y_n$. If the tail of the PDF of these variables decays faster than any power law, the PDF of the mth largest value drawn from each of M realizations of this sequence converge to the Gumbel class of stable distributions in the limit $M\to\infty$:

$$G_k(y) = K(e^{-\xi(y-s)}e^{-e^{-\xi(y-s)}})^m. \tag{14}$$

The distribution for the largest value in each realization ($m=1$) is often called the Fischer-Tippet-Gumbel (FTG) distribution. The FTG distribution with zero mean and unit variance requires $K=\xi=\pi/\sqrt{6}$ and $s=\gamma\sqrt{6}/\pi$, where $\gamma\approx 0.58$ is the so-called Euler constant.

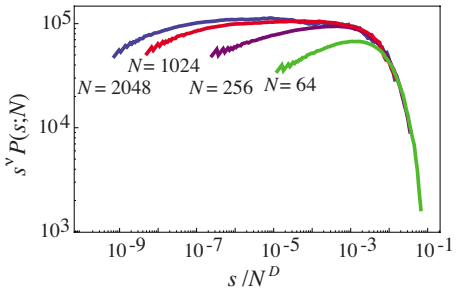

FIG. 6. (Color online) Attempted data collapse for the avalanches in the BTW model with respect to a threshold $\langle X\rangle/3$. We have plotted $s^{\nu-1}\int_s^\infty p_{\text{size}}(s')ds'$ as a function of s/L^D with $D=2.81$ for $N=64,256,1024,2048$.

A distribution obtained from the spin-wave approximation to the 2D XY model for equilibrium crititical fluctuations in a finite-size magnetized system is the so-called BHP distribution [13], which corresponds to Eq. (14) with k having the noninteger value $m=\pi/2\approx 1.57$. With $K=2.16$, $\alpha=1.58$, $\xi=0.93$, and $s=0.37$ this distribution has zero mean and unit variance. The difference between the normalized FTG and BHP distributions is rather small, and it is difficult to distinguish between the two based on experimental and numerical data.

Analysis of our simulations shows the claim that the toppling activity in strongly driven sandpiles has a PDF similar to the BHP or FTG distributions is wrong, unless the driving rate of the system is fine-tuned to some particular value. Actually, the normalized PDFs of the toppling activity are only insensitive to variation of the driving rate in the limits of weak and strong drives. In the limit of weak drive the PDFs are stretched exponentials as shown in Fig. 7, and in the limit of strong drive the PDFs are close to Gaussian.

Figure 8 shows the PDFs of the toppling activity in the strongly driven Zhang model where one unit ϵ of mass is fed

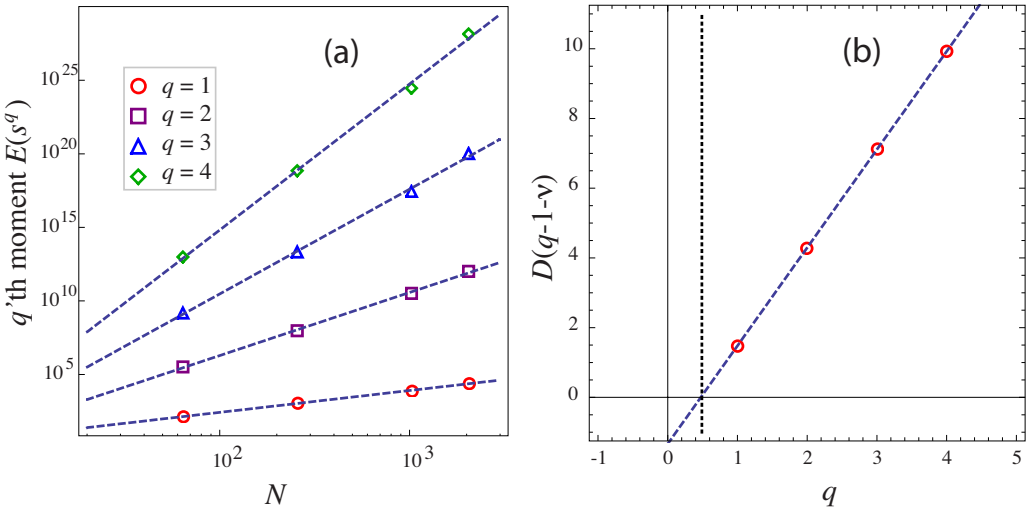

FIG. 5. (Color online) (a) The moments $\langle s^q\rangle$ plotted as functions of N for the size distribution of the BTW model with respect to a threshold $\langle X\rangle/3$. (b) The shape of the structure function $\zeta(q)$. The slope of the line is $D=2.81$ and the intersection with the first axis is $\nu-1=0.49$. This value is indicated by the dotted vertical line.

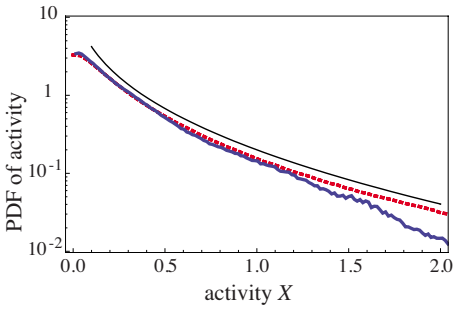

FIG. 7. (Color online) The PDF of the fluctuations in the toppling activity of the slowly driven BTW sandpile (thick solid curve) together with the corresponding PDF produced from the stochastic model (dashed curve). The thin solid curve is a stretched exponential fitted to the latter (slightly shifted vertically for visibility).

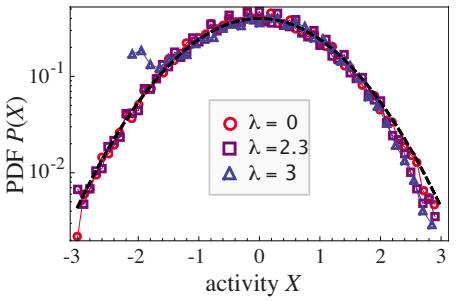

FIG. 8. (Color online) The PDF of the fluctuations in the toppling activity of the strongly driven Zhang sandpile for different values of λ (see text). The dashed curve is a fitted Gaussian.

at a random site at Poisson-distributed times. The intervals τ_f between two successive feeding events are then exponentially distributed $p_f(\tau_f)=\lambda^{-1}\exp(-\tau_f/\lambda)$, where $\lambda>1$ that the probability that a feeding event occurs at a given time step is λ^{-1}. The case $\lambda=0$ in Figure 8 stands for feeding at every time step. For $\lambda=0$ and $\lambda=2.3$ the sandpile is running, in the sense that avalanches never terminate. For $\lambda=3$, the sandpile is no longer running, and we see a deviation from the Gaussian shape in the left tail of the PDF.

The Gaussian PDFs for strongly driven sandpiles can actually be explained in terms of the stochastic model in Eq. (2). The idea is that the range of fluctuations is confined by the drift term $f(X)$, which now has a shape different from that of the slowly driven sandpile. Figure 9 shows the graph of both the diffusion coefficient $D(X)=\sigma^2X/2$ and the drift term for the strongly driven Zhang model. The diffusion coefficient has the same form as for the slowly driven sandpile, whereas the drift term is well approximated by a parabola: $f(X)=-aX^2+bX+c$. As explained in Sec. I this drift term confines the fluctuations in toppling activity to a bounded region around the positive root X_c of $f(X)$.

Due to the higher rate of random feeding, the memory effects described by the Hurst exponent $H\neq 1/2$ becomes inessential in the strongly driven sandpile, allowing us to give an approximate description of the time-dependent PDF through the Fokker-Planck equation

$$\frac{\partial P}{\partial t}=-\frac{\partial}{\partial X}[f(X)P]+\frac{\sigma^2}{2}\frac{\partial^2}{\partial X^2}(XP). \tag{15}$$

Stationary solutions of this equation must satisfy

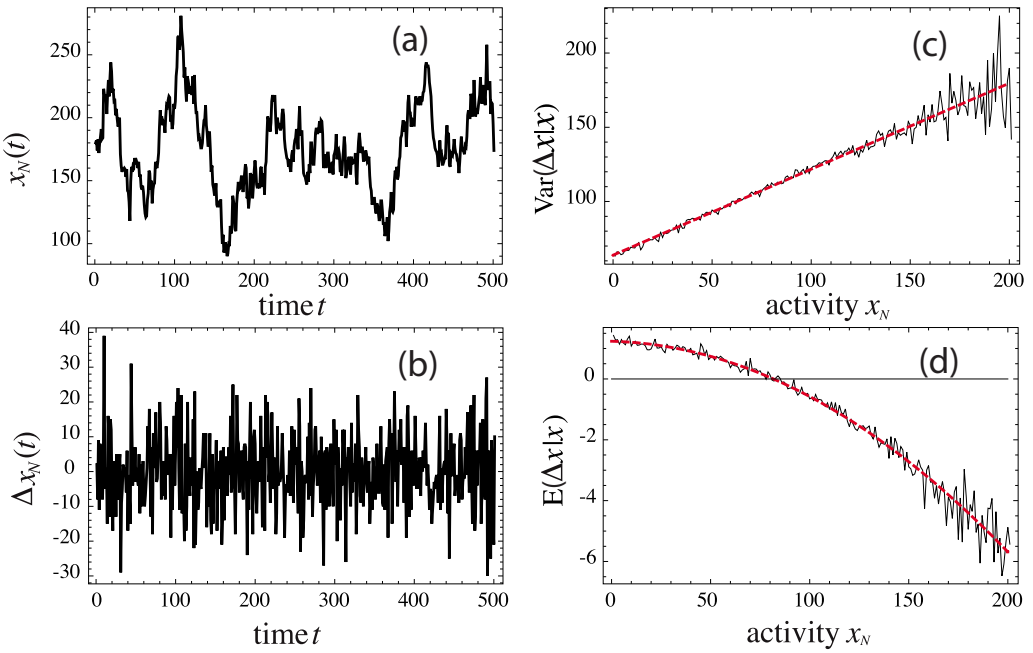

FIG. 9. (Color online) (a) Part of a time series for the toppling activity in a strongly driven Zhang sandpile. (b) The increments $\Delta x(t)=x(t+\Delta t)-x(t)$ of the signal in (a). The increments are large when the activity is large, as for the slowly driven case. (c) The conditional variance of the increments Δx given the value of x. The dashed line is a linear fit. (d) The conditional mean of increments. The dashed curve is a parabolic fit.

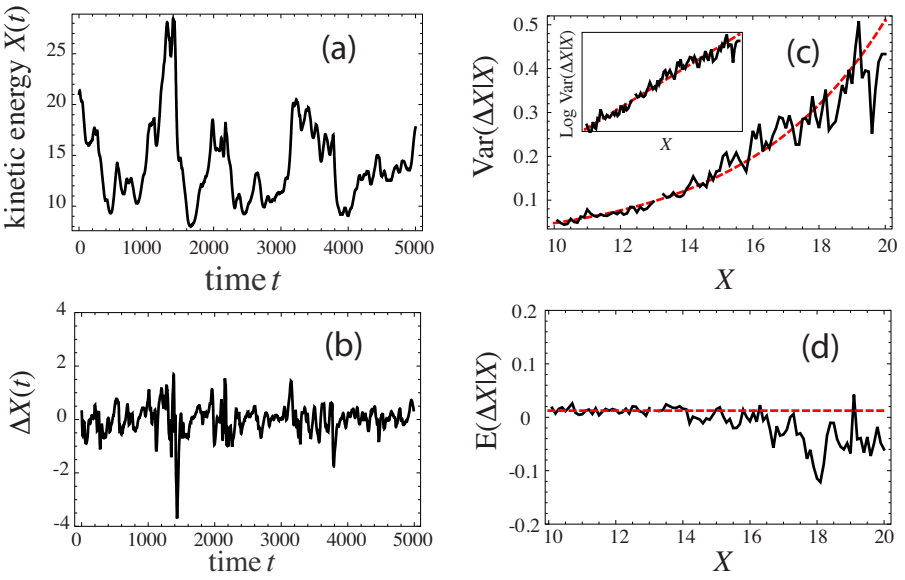

FIG. 10. (Color online) (a) Part of a time series for the kinetic energy in the 2D turbulence simulation. (b) The increments $\Delta X(t)=X(t+\Delta t)-X(t)$ of the signal in (a). As for the toppling activity in sandpiles, we see that the increments are large when the kinetic energy itself is large. (c) The conditional variance of the increments ΔX given the value of X. The dashed curve is a fitted exponential function. The inset shows the logarithm of this variance versus X (we have given no units on the axes or specified the base of the logarithm, since the only purpose is to show that the logarithm can be well fitted by a straight line). (d) The conditional mean of increments. We observe that the mean is approximately constant for a large range of X.

$$-\frac{d}{dX}[f(X)P]+\frac{\sigma^2}{2}\frac{d^2}{dX^2}(XP)=0,$$

and substituting $-aX^2+bX+c$ for $f(X)$, we have the Gaussian solution

$$P(X)=\frac{1}{\sqrt{2\pi}\Sigma}\exp\left(-\frac{(X-\mu)^2}{2\Sigma^2}\right),$$

with

$$\mu=\frac{b}{a} \quad \text{and} \quad \Sigma=\frac{1}{\sqrt{2}}\frac{\sigma}{a}.$$

To further substantiate that the toppling dynamics of sandpiles is fundamentally different from the fluctuating quantities that give rise to BHP and FTG distributions we apply the above analysis to the fluctuations in total kinetic energy in a simulation of two-dimensional Navier-Stokes turbulence. The two-dimensional geometry is chosen because of the inverse energy cascade in k space caused by merging of small vortices and formation of large structures, reminiscent of the formation of large avalanches emerging from the localized random perturbation in sandpile models. In the simulation, energy is injected via a source term on a characteristic, small spatial scale throughout the simulation area and is dissipated as loss through the open boundary.

We compute the conditional mean and conditional variance of the increment process. These results are presented in Fig. 10. We observe that contrary to the sandpile models, the diffusion coefficient for this process grows exponentially with X. Moreover, the drift term can be approximated by a small positive constant except when the kinetic energy is very large. This leads us to the stochastic differential equation (3), and the corresponding Fokker-Planck equation is

$$\frac{\partial P}{\partial t}=-b\frac{\partial P}{\partial X}+\frac{c^2}{2}\frac{\partial^2}{\partial X^2}(e^{2aX}P). \tag{16}$$

Stationary solutions of this equation must satisfy

$$-b\frac{dP}{dX}+\frac{c^2}{2}\frac{d^2}{dX^2}(e^{2aX}P)=0.$$

We can put $c=1$ without loss of generality and obtain the solution

$$P(X)=\frac{1}{\beta}e^{-(X-\mu)/\beta}e^{-e^{-(X-\mu)/\beta}},$$

where $\beta=1/2a$ and $\mu=(1/2a)\ln(1/2a)$. This is the standard FTG distribution. Figure 11 shows the normalized PDF for the fluctuations in total kinetic energy obtained from the fluid simulation along with a normalized FTG distribution and the PDF obtained from the simulation of Eq. (3).

VI. CONCLUSIONS

When output from simple models for avalanching systems are compared to observational data of real-world systems one has to deal with the problem of establishing a correspondence between the model variables and the observables of the natural system. In general, this is usually not an obvious task, since the model is usually not derived from first physical principles. The observation may be spatiotemporal, or just temporal. Likewise we may choose to analyze the spatiotemporal output from an avalanche model, or just some spatially integrated quantity like the total activity variable in

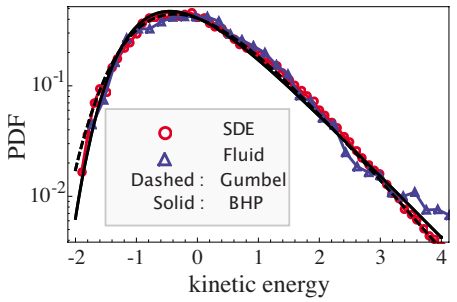

FIG. 11. (Color online) The normalized PDF for the fluctuation of kinetic energy in the 2D turbulence simulation together with a normalized FTG PDF (smooth solid curve), the normalized BHP PDF (smooth dashed curve) and a PDF obtained from the simulation of Eq. (3) (dotted curve).

a sandpile, presented as a time series. In this paper we have focused on the latter and, in particular, on reproducing the statistical properties of such time series by modeling the stochastic process by means of a stochastic differential equation.

Since our interest is avalanching dynamics, we focus on avalanche statistics, and we have to face the problem of how to define what an avalanche is when our observational data is in the form of a time series. In general, we cannot expect that such a definition is necessarily equivalent to a definition based on spatiotemporal data, at least not in those cases where feeding of new "sand grains" occurs while avalanches are running. In those cases several spatially separated avalanches may run simultaneously, but these cannot be separated in a purely temporal analysis. For such a continuously driven model system the temporal signal may never be zero, and in an observational time series noise also makes it impossible to use a zero-signal condition to separate an avalanching state from a quiet state. Thus, the natural way out is to define the avalanching state by means of a threshold level on the activity signal, giving rise to the concept of type-II avalanches.

In this paper we have shown that the toppling activity in sandpiles, and also global kinetic energy in a 2D fluid simulation, can be modeled by stochastic differential equations. The modeling clarifies that the main discrepancy between the mean-field approach and the actual BTW and Zhang models is related to the Hurst exponent of the activity process, which is different for the two sandpile models. It also clarifies the origin of the differences between the scaling exponents for type-I and type-II avalanches, and why type-II avalanches exhibit clearer scaling characteristics than type-I avalanches.

It follows from the theory how to rescale coordinates to approach the thermodynamic limit, and the results obtained for finite-size scaling in the BTW model in Sec. IV give a strong indication that this limit actually exists.

For continuously driven sandpiles the stochastic equation can be cast into a Fokker-Planck equation due to the loss of memory caused by the random feeding. This allows an analytic solution for the activity PDF, which is a Gaussian for the sandpile models, but gives rise to the FTG distribution for the 2D fluid simulation. These results show that the non-Gaussian universal PDF described in [12,13] is not relevant for strongly driven sandpiles, but may be so for certain turbulence models. The stochastic theory relates the difference between Gaussian- and FTG-distributed activity signals to the difference between a linear and exponential X dependence of the diffusion coefficient in the stochastic equation.

[1] P. Bak, C. Tang, and K. Wiesenfeld, Phys. Rev. Lett. **59**, 381 (1987).
[2] Y.-C. Zhang, Phys. Rev. Lett. **63**, 470 (1989).
[3] K. Christensen and N. Moloney, *Complexity and Criticality* (Imperial College Press, London, 2005).
[4] H. J. Jensen, *Self-Organized Criticality* (Cambridge University Press, Cambridge, England, 1998).
[5] M. Rypdal and K. Rypdal, e-print arXiv:0710.4010v1.
[6] M. Paczuski, S. Boettcher, and M. Baiesi, Phys. Rev. Lett. **95**, 181102 (2005).
[7] B. Øksendal, *Stochastic Differential Equations: An Introduction with Applications* (Springer, Berlin, 2000).
[8] E. V. Ivashkevich and V. B. Priezzhev, Physica A **97**, 254 (1998).
[9] M. Ding and W. Yang, Phys. Rev. E **52**, 207 (1995).
[10] A. Carbone, G. Castelli, and H. E. Stanley, Phys. Rev. E **69**, 026105 (2004).
[11] N. Watkins *et al.*, e-print: arXiv:0803.2833v1.
[12] S. T. Bramwell, P. C. W. Holdsworth, and J.-F. Pinton, Nature (London) **396**, 552 (1998).
[13] S. T. Bramwell, K. Christensen, J. Y. Fortin, P. C. W. Holdsworth, H. J. Jensen, S. Lise, J. M. Lopez, M. Nicodemi, J. F. Pinton, and M. Sellitto, Phys. Rev. Lett. **84**, 3744 (2000).
[14] E. J. Gumbel, *Statistics of Extremes* (Dover, Mineola, NY, 1958).
[15] S. Coles, *An Introduction to Statistical modeling of Extreme Values* (Springer, Bristol, 2001).
[16] K. Christensen and Z. Olami, Phys. Rev. E **48**, 3361 (1993).